

Interpretation of long-range interatomic force

A. Buldum and S. Ciraci

Department of Physics, Bilkent University, Bilkent 06533, Ankara, Turkey

C. Y. Fong

Department of Physics, University of California, Davis, Davis, California, 95616-8677

J. S. Nelson

Semiconductor Physics Division, 1112, Sandia National Laboratories, Albuquerque, New Mexico 87185-5800

(Received 8 June 1998; revised manuscript received 15 September 1998)

Recent direct mechanical measurements of atomic force microscopy showed that the force between the silicon tip and the silicon sample is long range in the attractive region and its magnitude at maximum is relatively smaller. These features disagree with previous theoretical predictions based on the *ab initio* calculations. We investigated the nature of forces between a silicon tip and the silicon (111)-(2×1) surface by performing first-principles pseudopotential and classical molecular dynamics calculations and by calculating the van der Waals interaction. The first two methods give forces that are short range in nature. Fair agreement between the experiment and theory is obtained when the van der Waals interaction is included. The effect of the tip induced deformation is analyzed. [S0163-1829(99)04504-X]

I. INTRODUCTION

The nature and range of tip-sample interactions in scanning tunneling microscopy (STM) and atomic force microscopy¹ (AFM) have been addressed by several experimental and theoretical studies.²⁻¹¹ *Ab initio* calculations^{3,5,7} based on the self-consistent field (SCF) pseudopotential method within the local density approximation have yielded the interaction (or adhesion) energy E in the range of ~ 1 eV for the equilibrium separation between a sharp metal tip and sample. The maximum attractive force for the same tip-sample system that was calculated¹² self-consistently within the Hellmann-Feynman theorem was found to be ~ 2 nN. The interaction between a metal tip and graphite (semimetal) surface was weaker, so relatively smaller adhesion energy and the tip force were calculated.⁵ It was also shown that the attractive force does not increase additively if the single atom tip is replaced by a cluster of atoms.⁵ However, regardless of the type of material, the tip-sample interaction due to the Coulomb interaction between electrons and ions (and hence due to overlap of the sample and tip wave functions) decays exponentially. Therefore it is short range. The range of this attractive force F_{SR} may change when the tip-induced relaxation of atoms is taken into account. In addition to the short-range forces, the contribution of the long-range forces, such as the van der Waals (vdW) interaction, has been questioned.⁸⁻¹¹ Calculations based on the Lifshitz asymptotic expression^{13,14} have indicated that the vdW force F_{vdW} is weak for a large tip-sample separation d and for a conical tip with a small semiangle. However, F_{vdW} being a weak body force can be significant for a blunt or spherical tip with separation not far from the sample ($d \sim 15 - 20$ Å).

The force variations $F_{expt}(d)$, measured by AFM, have displayed features that are rather different from early theoretical results summarized above.³⁻⁶ For example, $F_{expt}(d)$ between the gold tip and Ni surface showed a long-range

attractive region;⁹ a significant attractive force ($F_{expt} \sim 1$ nN) was recorded even for $d \sim 300$ Å. The attractive force increased to 25 nN for $d \sim 50$ Å. The longer range of the attractive force is in strong disagreement with *ab initio* force calculations since the calculated value of the short-range force $F_{SR}(d)$ becomes negligible for $d \sim 7$ Å. In order to explain the long-range attractive force with significant magnitude several types of force having different origins were proposed.⁹ Recently, Jarvis *et al.*¹⁵ reported their results on the direct mechanical measurements of the interatomic potential by using a modified atomic force microscope equipped with a magnetically controlled feedback mechanism, whereby the cantilever is prevented from jumping to contact. This way, one was able to measure the interaction energy until a small separation. This measured interaction between the Si tip and the Si(111)-(2×1) surface was, however, rather different from the theoretical predictions, as well as from the AFM results obtained earlier for the diamond tip and sample.⁹ In particular, the range of the interaction energy $E_{expt}(d)$ and the tip force $F_{expt}(d)$ that was obtained from the stiffness measurement by integration were much longer than the range of $F_{SR}(d)$ calculated for metals by using *ab initio* methods.⁷ For example, the attractive tip force varied from approximately 0.1 nN to 0.3 nN as a result of the tip approach of 20 Å. Moreover, unlike the earlier measurements,⁹ the magnitude of $F(d)$ was small and had the maximum value ~ 0.3 nN.

The present work aims to provide an understanding of the unusual variation of attractive force measured¹⁵ between the Si tip and the Si(111)-(2×1) sample. The source of disagreement with earlier studies is sought in the materials of the tip and sample, tip structure, and forces of different origins that may contribute to the resultant attractive force. To this end, we first calculate the short-range force variation F_{SR} for the same tip-sample system by using the SCF pseudopotential method. Since the atomic configuration at

the apex of the tip cannot be controlled, small asperities can form contacts with the sample near the maximum of $F_{expt}(d)$. Consequently, one expects that the local deformation and the repulsive force generated at the contact can affect the range and the magnitude of the total attractive force $F_{expt}(d)$. To reveal the effect of the local deformation on the tip force we simulated also a Si(111) tip approaching the Si(111)-(2×1) surface by using a molecular dynamics method. The variation of the atomic configuration and the resulting tip force are calculated as a function tip displacement s . Since the vdW interaction can be significant and responsible for the long-range attractive force,⁸ we determine the Hamaker constant for the Si tip and the Si sample and calculate the vdW force for various Si tips having different size and shape. Finally, we combine the results of the above calculations to analyze the experimental force variation.

II. *Ab initio* CALCULATIONS

The Coulomb interaction between the tip and sample diminish at large separation owing to the complete shielding of the charges. As d decreases, the wave functions start to overlap, resulting in an attractive interaction. The interaction energy $E_{SR}(d)$ is obtained by subtracting the total energies of isolated tip and sample from the total energy of the tip-sample system separated by d . Then the force $F_{SR} = -\partial E_{SR}/\partial d$, or by using the Hellmann-Feynman theorem

$$\vec{F}_{SR}(d) = - \sum_j \langle \nabla_{\vec{\tau}_j} H_{LDA} \rangle, \quad (1)$$

$\vec{\tau}_j$ being the position vectors of the tip atoms. Once the self-consistency has been achieved, changes in the wave function due to the displacement of the nuclei do not contribute to the force since the eigenfunctions are obtained variationally.¹⁶

As a consequence, \vec{F}_{SR} can be expressed as the sum of the electron mediated attraction^{8,12} (in which the electron density is calculated from the self-consistent wave functions) $\int (\partial/\partial \vec{\tau}_j) [Z_j/|\vec{\tau}_j - \vec{r}|] [\rho_s(\vec{r}) + \Delta\rho(\vec{r})] d\vec{r}$ and the ion-ion repulsion $-\sum_s (\partial/\partial \vec{\tau}_j) [Z_j Z_s/|\vec{\tau}_j - \vec{\tau}_s|]$. Here $\vec{\tau}_s, \rho_s(\vec{r}), \Delta\rho(\vec{r}), Z_j$ and Z_s are, respectively, the positions vectors of the sample atoms, the charge density of bare sample, the net change in charge density due to the tip-sample interaction, and the charge of the tip and sample ions. As d increases the attractive force decays exponentially and is canceled by the repulsive force. It is also shown¹⁷ that $F_{SR} \sim -\Sigma \partial M/\partial d$, M being the tunneling matrix between the tip and sample wave functions. In the present study, $E_{SR}(d)$ is calculated by using complete nonlocal pseudopotentials given in the Kleinman-Bylander form¹⁸ and the Ceperley-Adler¹⁹ exchange-correlation potential. The pyramidal tip has a single atom at the apex that is stacked in Si(111) planes; it is represented by seven Si atoms. The substrate has the π -bonded Si(111)-(2×1) structure and consists of four layers or 32 Si atoms in the cell. The tip-sample system is treated by the supercell structure with a negligible interaction between adjacent cells; each cell contains 39 Si atoms. The kinetic energy cutoff is taken to be $|k+G|^2 \leq 12$ Ry, so the electronic states are expressed by the linear combination of ~ 1200 plane waves. The relaxations of the atoms under the tip-sample interaction are not taken into

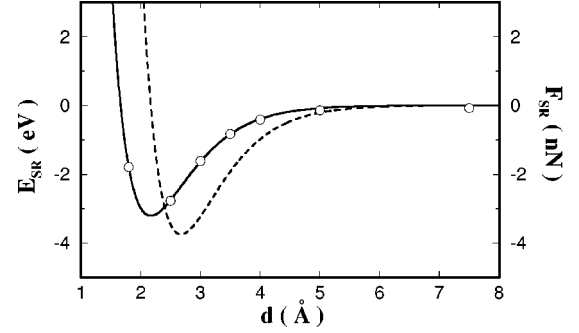


FIG. 1. Variation of the interaction energy E_{SR} (solid line) and short range force F_{SR} with the tip-sample separation d calculated by the self-consistent field pseudopotential method. The tip and sample are assumed to be rigid.

account. This is a reasonable approximation for the present study, which aims to reveal the range of F_{SR} at large d , but it is not valid for small d where a strong attractive or repulsive interaction can lead to significant elastic and plastic deformation. The effect of deformation on the force variation will be investigated by using much larger number of atoms and by performing molecular dynamics calculations in Sec. III.

Figure 1 illustrates the variation of the interaction energy $E_{SR}(d)$, calculated self-consistently within the local density approximation, and force $F_{SR}(d)$ derived therefrom. The maximum attraction is ~ 3.2 eV at $d \sim 2.1$ Å and it decays and becomes negligible for $d > 6.5$ Å. The maximum attractive force is 3.9 nN and occurs for $d \sim 2.7$ Å; this value is much larger than the maximum of $F_{expt}(d)$.¹⁵ In the present work the Si tip is sharp and has a single atom at the apex, whereas the atomic structure of the apex is not characterized and the possibility that the tip may have more than one atom at the apex is not ruled out. So the discrepancy $\max\{F_{expt}(d)\} - \max\{F_{SR}(d)\}$ would grow if we were using a blunt tip in our calculation. Clearly, the range of F_{SR} is rather short and cannot contribute to the measured long-range attractive force if $d > 8$ Å.

Earlier, Perez *et al.*²⁰ investigated the interaction between the Si(111)-(5×5) surface and the sharp tips stacked in Si(111) planes that have a single atom at the apex. They carried out fully relaxed *ab initio* calculations for the tip moving at a constant height (with $d = 5$ Å) above the surface and obtained the corrugation of $E_{SR}(x)$ and $F_{SR}(x)$ (x being the displacement parallel to the surface). They concluded that the single Si atom at the apex of the tip that has a dangling bond directed towards the surface yields high resolution (or high corrugation) and is due to the covalent bond forming even for $d = 5$ Å. This actually corroborates an earlier theory^{3,21} proposing tip-induced states that enhance the STM images. The tip structure used in the present work is reminiscent of the hydrogen saturated tetrahedral tip with 4 Si atoms used by Perez *et al.*; both tip structures allow a dangling bond to form at the apex atom. We terminated 3 Si atoms behind the apex atom by 3 additional Si atoms (instead of 3 hydrogen atoms) as a continuation of the tetrahedral bonding since one needs to use more plane waves to describe the Si-H bonds. Also the tip-induced deformation leads to effects on the value of calculated short-range force that can be negligible at $d = 5$ Å. As expected, the force

value calculated by Perez *et al.*²⁰ in fair agreement with our results of $F_{SR}=0.25$ nN at $d=5$ Å.

III. MOLECULAR DYNAMICS CALCULATIONS

The effects of the tip-sample interaction and the deformation induced therefrom are investigated by using a tip-sample system comprising 1367 Si atoms. In the present case, the tip and the sample have the same atomic structure, but involve more atoms and become more extended as compared to the model used in the above *ab initio* calculations. The substrate is made by ten Si(111) layers (hence 1200 atoms) with the 2×1 reconstruction geometry leading to the π -bonded chain structure and fivefold and sevenfold rings at the surface. The sharp and pyramidal tip has 167 Si atoms that are arranged in the Si(111) layers. The top two layers of the tip and the bottom two layers of the substrate are taken to be robust. The rest of the atoms (111 tip and 960 substrate atoms) are subject to relaxation under the tip-sample interaction. These atoms are specified as dynamic atoms. The tip-sample system is treated by the periodic boundary condition, where each substrate layer includes 6×10 Si(111)-(2×1) cells. The interaction between the atoms are calculated by using the Stillinger-Weber²² potential, which has had reasonable success in predicting the bulk defects and the reconstruction of silicon surface with coordination number lower than that in the bulk.²³ It is also used to investigate the stick-slip behavior and wear between a Si tip and the Si surface with a noncrystalline contact.²⁴ We note that the cutoff distance for the three-body interaction is only 3.6 Å in the Stillinger-Weber potential²² and hence the interaction is short range. For that reason the calculated energy and force are specified by the subscript *SR*. Starting from a large spacing (5.5 Å), the two robust layers of the Si tip are displaced towards the sample in increments of $\Delta s=0.05$ Å, whereas the total displacement at the end of n steps is $s=n\Delta s$. Between two consecutive steps of displacements, all dynamic atoms are relaxed for 2000 time steps. In each time step²⁵ of $\Delta t=3.8 \times 10^{-16}$ s, the dynamic atoms are allowed to move under the forces calculated at the beginning of the time step. At the end of each time step, the system is thermalized to 4 K. That the number of relaxation steps is suitable for the equilibration of the tip-sample system following a 0.05 Å approach of the tip is tested by calculating the temperature and potential energy variations.

Figure 2 shows the calculated energy and force variations with the displacement s of the tip approaching from a large spacing d . Figures 2(a) and 2(c) correspond to the tip facing an atom of the π -bonded chain of the substrate surface (i.e., the top site *T*) and Figs. 2(b) and 2(d) are for the tip facing the center of the hexagon on the surface of the substrate (i.e. the hollow site *H*). We note that the total energy of the system decreases discontinuously with s . By averaging the $E_{SR}(s)$ curve one can distinguish the steps C_1, C_2, C_3 , where the total energy makes sudden falls. At the same points the tip force also decreases suddenly. Sudden changes in the $E_{SR}(s)$ and $F_{SR}(s)$ curves are related to the structural transitions at the contact where a double Si(111) layer of the sharp tip is included to the noncrystalline contact as shown in Fig. 3. This way the boundary separating the ordered

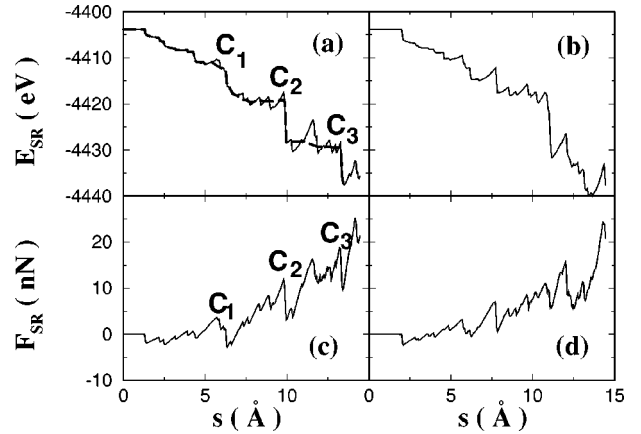


FIG. 2. Variation of the interaction energy E_{SR} , (a) and (b), and the force F_{SR} , (c) and (d), with the displacement of the tip s , calculated using classical molecular dynamics. (a) and (c), and (b) and (d), correspond to the apex of the tip facing the top site and the hollow site, respectively. C_1, C_2 , and C_3 indicate structural transitions.

structure of the tip from the noncrystalline neck at the contact advances discontinuously towards the shank with increasing s . A similar force variation has been obtained in the calculations simulating the nanoindentation, as well as the tip retracting from a nanoindentation.^{26–29} It is also observed experimentally.^{27,30} Extensive analysis²⁹ of the force variation found the local structural changes (for example, the order-disorder transition) responsible for the standard behavior displaying sudden jumps such as C_1, C_2 . In the course of indentation both the tip and the surface are deformed. While the deformation at the apex of the tip is severe due to the relatively small coordination number of the atoms, the sur-

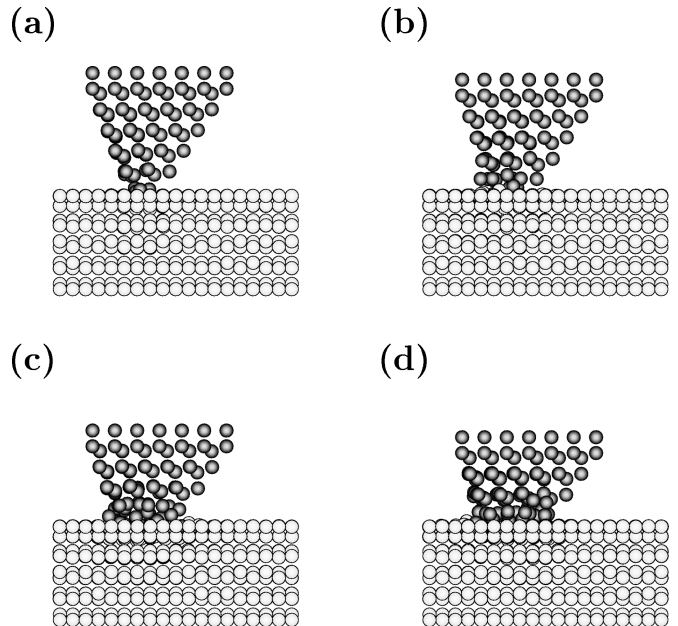


FIG. 3. Snapshots of the atomic structure of the tip approaching the sample. (a) and (b) correspond to the atomic configuration before and after the structural change denoted C_1 takes place. (c) and (d) are the same for C_2 . The deformation of the sample surface is not seen in the side view.

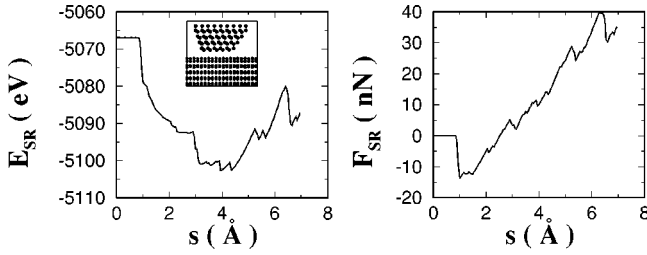


FIG. 4. Variation of the interaction energy E_{SR} and the force F_{SR} with the displacement s calculated for a blunt tip. The inset shows the blunt tip before the contact.

face at the contact is deformed only locally. (The latter is not seen clearly in the side view in Fig. 3.) Practically, the sharp tip is crushed on the sample surface. The reverse situation can occur if a blunt and hard tip were pressed into a softer sample.^{27,31}

The behavior of the deformation outlined above demonstrates that depending on the shape of the tip, the force variation with s can be rather different from Fig. 1. In the present case, while the atoms at the apex form a contact and enter the repulsive force region, the second layer atoms can still be attracted by the substrate. Accordingly, the measured tip force is the resultant of the attractive as well as repulsive force acting at different regions of the tip. Depending on the material parameters, the shape, and the atomic structure of the tip, F_{SR} can be occasionally and temporarily repulsive. Here we address an important issue, namely, the response of the cantilever to the actual force variation (or stiffness variation). Each structure of the molecular dynamics simulations corresponds to a time interval $\sim 10^{-13}$ s, while the response time of a cantilever is usually larger than $\sim 10^{-9}$ s. Therefore, several structures occurring in atomic simulations cannot be sensed by the cantilever. In this respect, the force variation $F_{expt}(d)$ obtained by the integration of the averaged stiffness may deviate from the actual force variation.

If the tip is blunt but comprises several asperities in different levels, the range of force can be even longer than displayed in Figs. 2(c) and 2(d). On the other hand, $E_{SR}(s)$ and $F_{SR}(s)$ of an atomically flat tip (without asperity) have a shorter range than those of the sharp tip (see Fig. 4). This demonstrates the crucial effect of the deformation leading to atomic rearrangements. Since the jump to the contact is avoided in the experiments by Jarvis *et al.*,¹⁵ the discussion in this section may not be directly related to $F_{expt}(d)$. However, the present study demonstrates that the tip-induced deformation modifies the range of the net tip force in spite of the short-range interatomic force. As a result, $F_{expt}(s)$, as well as $F_{SR}(s)$, where the tip and sample atoms are allowed to relax, differs from $F_{SR}(d)$ in Fig. 1; the range of the attractive $F_{expt}(s)$ or $F_{SR}(s)$ in Fig. 2(c) or 2(d) is extended.

IV. van der WAALS INTERACTION

The van der Waals interaction occurs as a dipole-dipole interaction^{13,14} even if two electrodes (tip and sample) are well separated and become completely decoupled. The importance of the vdW interaction in STM and AFM was recognized earlier^{5,8,10,11} and it was argued that depending on the overall shape of the tip support, the atom at the apex of

the tip can experience strong repulsion, even leading to irreversible deformation, while an atom farther away from the apex experiences an overall attraction. The measured force¹⁵ that exhibits a longer range has led us to examine the vdW interaction between the Si tip and the Si sample. The calculation of the vdW potential might be easier if the interaction is assumed to be nonretarded and additive. Then, only the Hamaker constant A remains to be determined for the pair of materials to evaluate the integral of the pair potential of the form $-C/r^6$. Here C is calculated from A and depends on the materials of the tip and sample. However, the additivity breaks down when the presence of any other atom may change the polarizability of a pair of atoms. The Lifshitz theory¹³ redefines the Hamaker constant considering this complexity. Since the relevant d in the experiment¹⁵ is rather large, the asymptotic interaction expression for a polarizable surface and single atom can be used safely. In this case, the interaction energy E_{vdW} is given by summing $-C/\tau_j^3$ over the Si tip. In our study we first focus on the determination of the Hamaker constant for the Si tip and the Si sample and then perform the calculation of the vdW force between the tip and the sample.

The expression for the Hamaker constant can be calculated from the spectral relation¹⁴

$$A \approx \frac{3h}{8\pi^2} \int_{\omega_1}^{\infty} \left(\frac{\epsilon(i\omega) - 1}{\epsilon(i\omega) + 1} \right) d\omega. \quad (2)$$

Here ϵ is the dielectric constant of Si. For the determination of the Hamaker constant by using Eq. (2), the variation of the dielectric permittivity as a function of imaginary frequency has to be known. A model for $\epsilon(\omega)$ and $\epsilon(i\omega)$ for dielectric or nonconducting materials was introduced³² by using the assumption that oscillations of the charge density of these materials behave like a single oscillator with a main absorption frequency in the UV region. For conducting materials, the expression $\epsilon(\omega) = 1 - \omega_p^2/\omega^2$ can be used, where ω_p is the plasma frequency. Then the dielectric permittivity for imaginary frequencies becomes $\epsilon(i\omega) = 1 + \omega_p^2/\omega^2$. Plasma oscillations in the valence band are considered to be the source of the van der Waals interaction between silicon objects.³³ By using the plasma frequency of silicon³⁴ approximately $3.87 \times 10^{15} \text{ s}^{-1}$, we determined the Hamaker constant for the Si tip-sample system ($A \approx 0.34$ aJ) from Eq. (2). Then the constant in the Lifshitz asymptotic expression is equal to $A/\rho^2 \pi^2$; ρ is the atomic density of Si.

French *et al.*³⁵ assumed that the major source of the vdW interaction is interband excitation and is calculated to be $A = 0.21$ aJ. On the other hand, the value they obtained for the Hamaker constant by using the Tabor-Winterton approximation¹⁴ is rather large, $A = 0.67$ aJ. Accordingly, the vdW force illustrated in Fig. 5 would be reduced by 38% if one were to use the first value obtained from the spectral method; in contrast, it would increase by 93% if the value obtained from the Tabor-Winterton approximation were used. On the other hand, Perez *et al.*²⁰ used $A = 0.19$ aJ as determined by Senden and Drummond³⁶ in their recent calculation of the long-range force. Note that the calculated values of the Hamaker constant range in the interval $0.19 \text{ aJ} \leq A \leq 0.67$ aJ, depending on the type of excitation taken to

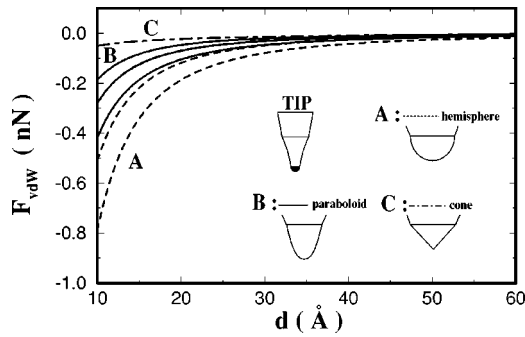


FIG. 5. van der Waals force F_{vdW} versus tip-sample separation d calculated for different types of tip apex shown in the inset.

be responsible for the vdW interaction. The value $A = 0.34$ aJ we calculated lies near the center of the interval. Of course, the precise value of the Hamaker constant is essential for the calculation of F_{vdW} . However, once the uncertainties in determining the actual shape and size of the tip are taken into account, the Hamaker constant used in the present work is suitable to estimate the variation of the long-range force and hence to analyze the experimental data.

Figure 5 illustrates the variation of the tip force generated by the vdW interaction with the tip-sample separation. A characteristic shape of a commercial Si tip is described in the inset and F_{vdW} is calculated for different tip ends (a hemisphere, paraboloid, and cone) that are joined to the characteristic tip support. Two remarkable features of F_{vdW} in Fig. 5 are that (i) it is rather long range and attractive and (ii) it depends strongly on the shape and size of the tip. For $d \sim 25$ Å, while the short-range force F_{SR} generated by the overlap of the wave functions diminishes, the force due to the vdW interaction is significant and hence $0.2 < F_{vdW} < 0.7$ nN. The measured tip force F_{expt} lies within these limits. Since the shape and size of the tip end used in the experiment cannot be determined, we cannot calculate

$F_{vdW}(d)$ precisely. Nevertheless, the present calculation for a Si tip and the Si sample shows that the vdW interaction can be responsible for the long-range variation of the experimental tip force. We note that the asymptotic expression for F_{vdW} diverges as $d \rightarrow 0$ and it may not be accurate for small d .

V. CONCLUSIONS

The *ab initio* self-consistent pseudopotential calculations, atomic simulations based on the classical molecular dynamic method, and calculations of the van der Waals interaction yield a number of interesting results that are important for a better understanding of the measured force by AFM. The range of the attractive force F_{SR} originating from the interaction of wave functions is calculated to be approximately $7-8$ Å. In the absence of deformation, this range is independent of the geometry of the tip. On the other hand, the maximum of F_{SR} is ~ 3.9 nN, which is significantly larger than the maximum measured attractive force. Clearly, $F_{SR} \ll F_{expt}$ for $d < 7-8$ Å, but $\max|F_{SR}| \gg \max|F_{expt}(d)|$, so the calculated F_{SR} alone cannot explain the variation of the measured force at small d . The van der Waals interaction calculated for certain types of tip support and tip end can yield force variation in agreement with the measured variation. It appears that $F_{expt}(d) \approx F_{SR}(d) + F_{vdW}(d)$ for $d > 4-5$ Å. Similar long-range behavior can be obtained if a charge transfer between the tip and sample or a polarization of charge due to the electric field takes place. However, we presume that such a situation is ruled out in the experiment. The serious discrepancy between the maximum values of the calculated F_{SR} and F_{expt} , however, remains unanswered. We do not provide a conclusive explanation why the maximum of the attractive force comes out so small in the experiment. It can be due to an effect that is not treated in the present study, perhaps related to the equipment measuring the stiffness. It appears that further experimental studies are required to illuminate this issue.

¹G. Binnig, C. F. Quate, and Ch. Gerber, Phys. Rev. Lett. **56**, 930 (1986).

²C. M. Soler, A. M. Baro, N. Garcia, and H. Rohrer, Phys. Rev. Lett. **57**, 444 (1986).

³S. Ciraci and I. P. Batra, Phys. Rev. B **36**, 6194 (1987).

⁴F. Abraham, I. P. Batra, and S. Ciraci, Phys. Rev. Lett. **60**, 1314 (1988).

⁵S. Ciraci, A. Baratoff, and I. P. Batra, Phys. Rev. B **41**, 2763 (1990); **42**, 7618 (1990).

⁶J. B. Pethica and A. P. Sutton, J. Vac. Sci. Technol. A **6**, 2490 (1988).

⁷*Basic Concepts and Applications of Scanning Tunneling Microscopy and Related Techniques*, Vol. 184 of *NATO Advanced Study Institute, Series E: Applied Sciences*, edited by H. Rohrer, N. Garcia, and J. Behm (Kluwer, Amsterdam, 1990); *Forces in Scanning Probe Methods*, Vol. 286 of *NATO Advanced Study Institute, Series E: Applied Sciences*, edited by H.-J. Güntherodt, D. Anselmetti, and E. Meyer (Kluwer, Amsterdam, 1995).

⁸S. Ciraci, E. Tekman, A. Baratoff, and I. P. Batra, Phys. Rev. B **46**, 10 411 (1992); S. Ciraci, E. Tekman, M. Gökçedağ, I. P.

Batra, and A. Baratoff, Ultramicroscopy **42-44**, 163 (1992).

⁹N. A. Burnham, R. J. Colton, and H. M. Pollock, Nanotechnology **4**, 64 (1993).

¹⁰U. Dürig, O. Züger, and D. W. Pohl, Phys. Rev. Lett. **65**, 349 (1990); U. Dürig and O. Züger, Vacuum **41**, 382 (1990); F. O. Goodman and N. Garcia, Phys. Rev. B **43**, 4728 (1991).

¹¹U. Hartmann, Phys. Rev. B **43**, 2404 (1991).

¹²See for example, I. P. Batra, S. Ciraci, G. P. Srivastava, J. S. Nelson, and C. Y. Fong, Phys. Rev. B **34**, 6632 (1988).

¹³E. M. Lifshitz, Zh. Éksp. Teor. Fiz. **29**, 94 (1956) [Sov. Phys. JETP **2**, 73 (1956)].

¹⁴J. N. Israelachvili, *Intermolecular and Surface Forces* (Academic, London 1985).

¹⁵S. P. Jarvis, H. Yamada, S. I. Yamamoto, H. Tokumoto, and J. B. Pethica, Nature (London) **384**, 247 (1996).

¹⁶J. C. Slater, J. Chem. Phys. **57**, 2389 (1972).

¹⁷F. Flores, A. M. Rodero, E. C. Goldberg, and J. C. Duran, Nuovo Cimento D **10**, 303 (1988); C. J. Chen, J. Phys.: Condens. Matter **3**, 1227 (1991).

¹⁸D. R. Hamann, Phys. Rev. B **40**, 2980 (1989); L. Kleinman and D. M. Bylander, Phys. Rev. Lett. **48**, 1425 (1982).

- ¹⁹D. M. Ceperley and B. J. Adler, Phys. Rev. Lett. **45**, 566 (1980).
- ²⁰R. Perez, M. C. Payne, I. Stich, and K. Terakura, Phys. Rev. Lett. **78**, 678 (1997).
- ²¹E. Tekman and S. Ciraci, Physica **38**, 486 (1988).
- ²²F. H. Stillinger and T. A. Weber, Phys. Rev. B **31**, 5262 (1985).
- ²³F. Abraham, I. P. Batra, and S. Ciraci, Phys. Rev. B **35**, 9552 (1987); Phys. Rev. Lett. **60**, 1314 (1988); F. F. Abraham and I. P. Batra, Surf. Sci. **163**, L752 (1985).
- ²⁴U. Landman, W. D. Luedke, and A. Nitzan, Surf. Sci. **210**, L177 (1989).
- ²⁵Note that the time steps of $\Delta t = 3.8 \times 10^{-16}$ s are appropriate for the Newtonian dynamics in the present study. Much longer Δt would lead to the jumps of atoms to local minima far from the global minimum. A similar simulation (see Ref. 24) has used time steps approximately one order of magnitude longer and increments Δs five times larger. Since the number of relaxation after each increment Δs can be arbitrarily large, the time interval $2000 \times \Delta t = 7.6 \times 10^{-13}$ s may not be a relevant time scale in the dynamics. For the critical discussion of the issue see also A. P. Sutton, Curr. Opin. Solid State Mater. Sci. **1**, 827 (1996).
- ²⁶A. P. Sutton and J. B. Pethica, J. Phys.: Condens. Matter **2**, 5317 (1990); J. A. Nieminen, A. P. Sutton, and J. B. Pethica, Acta Metall. Mater. **40**, 2503 (1992).
- ²⁷U. Landman, W. D. Luedke, N. A. Burnham, and R. J. Colton, Science **248**, 454 (1990).
- ²⁸T. N. Todorov and A. P. Sutton, Phys. Rev. B **54**, R14 234 (1996).
- ²⁹A. Buldum, S. Ciraci, and I. P. Batra, Phys. Rev. B **57**, 2468 (1998).
- ³⁰G. Rubio, N. Agrait, and S. Vieira, Phys. Rev. Lett. **76**, 2302 (1996); A. Stalder and U. Durig, Appl. Phys. Lett. **68**, 637 (1996).
- ³¹A. I. Livshits and A. L. Shluger, Phys. Rev. B **56**, 12 482 (1997); Ç. Kiliç, H. Mehrez, and S. Ciraci, *ibid.* **58**, 7872 (1998).
- ³²J. Mahanty and B. W. Ninham, *Dispersion Forces* (Academic, New York, 1976).
- ³³J. E. Inglesfield and E. Wikborg, J. Phys. F **5**, 1475 (1975); J. E. Inglesfield, *ibid.* **6**, 687 (1976).
- ³⁴C. Kittel, *Introduction to Solid State Physics* (Wiley, New York, 1986).
- ³⁵R. H. French, R. M. Cannon, L. K. DeNoyer, and Y. M. Chiang, Solid State Ionics **75**, 13 (1995).
- ³⁶T. J. Senden and C. J. Drummond, Colloids Surf., A **94**, 29 (1997).